Fc receptor engagement mediates differentiation of cardiac fibroblast precursor cells

Sandra B. Haudek*, JoAnn Trial*, Ying Xia*, Damon Gupta*, Darrell Pilling†, and Mark L. Entman*‡

*DeBakey Heart Center, Baylor College of Medicine and The Methodist Hospital, Houston, TX 77030; and †Department of Biochemistry and Cell Biology, Rice University, Houston, TX 77005

Communicated by Salih J. Wakil, Baylor College of Medicine, Houston, TX, May 23, 2008 (received for review March 27, 2008)

We previously described a critical role for a fibroblast precursor population in the development of a murine fibrotic cardiomyopathy model (I/RC). These precursors arose from circulating bone marrow-derived cells of monocytic origin. Administration of serum amyloid P (SAP) prevented the presence of this cell population in the heart and the cardiomyopathy. Because SAP binds to Fc receptors (FcRs) expressed on monocytes, we investigated the involvement of FcR signaling. We chose mice lacking the FcRγ chain protein (FcR$\gamma^{-/-}$), a common membrane-signaling component of activating FcRs. Like wild-type mice, FcR$\gamma^{-/-}$ mice developed fibrosis and cardiac dysfunction when subjected to I/RC. However, unlike wild-type mice, SAP in FcR$\gamma^{-/-}$ mice failed to inhibit the development of fibrosis and cardiac dysfunction and did not diminish the numbers of α-smooth muscle actin$^+$ and CD34$^+$, CD45$^+$ fibroblasts that were typical for I/RC. To further examine the role of SAP in monocyte-to-fibroblast transition, we performed *in vitro* assays in which human peripheral blood mononuclear cells (PBMCs) migrated through human umbilical vein endothelial cells (HUVECs). We found that MCP-1-dependent transendothelial migration of monocytes markedly accelerated their differentiation into fibroblasts. This monocyte differentiation to fibroblasts was eliminated when SAP was added to the PBMC suspension before endothelial transmigration. Adding SAP to cells after successful migration did not inhibit fibroblast maturation. These data indicate that SAP inhibits the differentiation of a blood-borne, myeloid cell population into fibroblasts by signaling through activating FcRs before transendothelial migration has occurred. We suggest that FcR activation of circulating precursor cells may represent a new treatment target for adverse remodeling and cardiac fibrosis.

endothelial transmigration | fibrosis | heart | monocytes | serum amyloid P

Collagen deposition is a critical pathogenic factor in the development of cardiac dysfunction (1). Because interstitial fibrosis is often found in dysfunctional myocardial segments from patients with ischemic cardiomyopathy (2), the role of fibrosis in the pathogenesis of this disease is recognized. However, the molecular mechanisms responsible for collagen deposition in the heart remain unknown (3).

In our previous work, we developed a murine model of closed-chest ischemia and reperfusion consisting of multiple, daily 15-min occlusions (I/RC) (4). This protocol induced prolonged up-regulation of monocyte chemoattractant protein 1 (MCP-1) and the development of interstitial fibrosis and myocardial dysfunction in the absence of myocyte cell death. When MCP-1 was deleted, I/RC caused no fibrosis or cardiac dysfunction (5). Further investigations demonstrated that the I/RC-induced MCP-1 expression resulted in the uptake of a bone marrow-derived, blood-borne fibroblast precursor population of hematopoietic origin (6). These precursors gave rise to a population of small, spindle-shaped fibroblasts that were highly proliferative and expressed α-smooth muscle actin (α-SMA), type I collagen, CD34 (a marker of precursor cells), and CD45 (hematopoietic cell marker). We further showed that daily administrations of serum amyloid P (SAP) to mice undergoing I/RC markedly reduced the appearance of activated fibroblasts in the heart despite an identical ischemic challenge (6). Also, cardiac fibrosis was virtually eliminated, and cardiac function and structure were preserved.

The best known ligands for SAP on mononuclear cells are receptors that bind to the Fc regions of IgG [Fc receptors (FcRs)] that are found on the surface of a variety of hematopoietic cells. Among IgG-binding FcRs, there are four distinct classes, all of which are expressed on peripheral blood mononuclear cells (PBMCs), albeit with different binding affinities for IgG subclasses and distinct cell activation/inhibition signaling pathways (see reviews in refs. 7 and 8). SAP is a ligand for activating FcRs (9). Most activating FcRs associate with a common membrane-signaling component termed FcRγ chain protein that contains an immunoreceptor tyrosine-based activation motif (ITAM) to exert their effects (7, 8).

In the study described here, we used two strategies to test the hypothesis that SAP exerts its effect on fibrosis through activation of FcRs on monocytes. First, we studied *in vivo* effects of I/RC in KO mice lacking the FcRγ chain protein (FcR$\gamma^{-/-}$ mice). In contrast to wild-type mice (6), we found that FcR$\gamma^{-/-}$ mice were not protected by SAP from developing the I/RC response. It also strongly suggested a role for SAP in modulating the monocyte-to-fibroblast transition through action on the FcRs. To better dissect this transition, we developed an *in vitro* model of monocyte-derived fibroblast formation using human cells. In these *in vitro* transendothelial migration (TEM) studies, we found that markedly accelerated monocyte differentiation into fibroblasts resulted from MCP-1-dependent transendothelial migration of monocytes. As in the animal model, SAP profoundly inhibited monocyte-to-fibroblast transition, but only if present before transendothelial migration.

Results

FcR$\gamma^{-/-}$ Mouse Model in I/RC. Because the current article represents an extension of our previous studies in wild-type mice, a direct comparison of previous wild-type data with current data on FcR$\gamma^{-/-}$ mice are summarized in Table 1. As is described in the remainder of this article, the ability of SAP to prevent adverse remodeling in I/RC requires the function of FcRγ.

Histology. To investigate the mechanisms of SAP inhibition *in vivo*, we used FcR$\gamma^{-/-}$ mice, which lack the FcRγ chain protein. In contrast to wild-type mice, in which SAP markedly inhibited I/RC-induced collagen deposition (6), we found that FcR$\gamma^{-/-}$ mice were not protected by SAP from fibrosis. As shown in Fig. 1*A*, collagen deposition in SAP-treated hearts was not different from that in diluent-treated hearts (5.6 $\pm$ 0.5 vs. 6.3 $\pm$ 0.5% area)

Author contributions: S.B.H., J.T., and M.L.E. designed research; S.B.H., J.T., Y.X., and D.G. performed research; D.P. contributed new reagents/analytic tools; S.B.H., J.T., and M.L.E. analyzed data; and S.B.H., J.T., and M.L.E. wrote the paper.

The authors declare no conflict of interest.

Freely available online through the PNAS open access option.

‡To whom correspondence should be addressed. E-mail: mentman@bcm.tmc.edu.

Table 1. Murine ischemia reperfusion cardiomyopathy (I/RC): Summary of previous and current results

Variable		Wild-type sham (4–6)	Wild-type I/RC (4–6)	Wild-type I/RC + SAP (6)	FcRγ$^{-/-}$ sham	FcRγ$^{-/-}$ I/RC	FcRγ$^{-/-}$ I/RC + SAP
Histology	Collagen	—	+++	+	—	+++	++++
	Myofibroblasts	—	+++	—	—	+++	+++
	Macrophages	—	+++	+++	—	++	++
Isolated cells	CD34$^+$	—	+++	—	—	+++	+++
	CD45$^+$	—	+++	++	—	++++	++++
	CD34$^+$/CD45$^+$	—	+++	—	—	++	++
	Proliferation	—	+++	—	—	+++	+++
	Morphology	big, flat	small, spindle	big, flat	big, flat	small, spindle	small, spindle
Function	% Fractional shortening	—	−−−	—	—	−−−	−−−
	% Anterior wall thickening	—	−−−	—	—	−−−	−−−

For better comparison, data from previously published studies (4–6) and the current study, which is a direct extension of the earlier ones, are summarized. Data are represented by symbols: —, baseline levels; +, activated levels; the amount of + is proportional to the extent of increase (histology and cell markers). Reduced function is measured by the number of −. Despite identical genetic background (C57BL/6), minor differences in absolute values between wild-type and FcRγ $^{-/-}$ mice existed, but these were independent of the presence or absence of SAP during I/RC.

(Fig. 1*A*). Similarly, SAP treatment of FcRγ$^{-/-}$ mice did not reduce the presence of I/RC-induced α-SMA$^+$ cells compared with nontreated I/RC animals (16.1 ± 3.1 vs. 17.9 ± 4.4 cells/mm^2) (Fig. 1*B*). This finding was in contrast to our previous I/RC studies using wild-type mice, in which α-SMA$^+$ cell number was reduced 6-fold by SAP when compared with nontreated wild-type mice (6). Also consistent with our previous data in wild-type mice (6), in FcRγ$^{-/-}$ mice, SAP did not affect the number of macrophages (100 ± 8 vs. 122 ± 11 cells/mm^2) (Fig. 1*C*) measured within the ischemic regions. These data indicate that SAP signaling through activating FcRs was necessary to inhibit monocyte-derived fibroblast differentiation and reduce fibrosis in the I/RC heart.

Analysis of Isolated Cell Populations. In FcRγ$^{-/-}$ mice undergoing I/RC, the percentage of CD34 (4.0 ± 0.4 vs. 3.8 ± 0.5%), CD45 (14.2 ± 2.3 vs. 14.8 ± 1.8%), and CD34/CD45 (1.1 ± 0.2 vs. 1.3 ± 0.3%) positive cells of all viable, noncardiomyocyte cells was not reduced by SAP treatment (Fig. 2*A*), which was in contrast to previous studies in wild-type mice (6). Moreover, cardiac fibroblasts cultured from both SAP and diluent-treated I/RC-FcRγ$^{-/-}$ mice consisted of many small spindle-shaped cells, so the morphological characteristics of the cell population were not altered by SAP (Fig. 2*B*). Similarly, in FcRγ$^{-/-}$ mice, SAP treatment did not reduce the rapidly proliferative cell population seen after I/RC (3.5 ± 0.5 vs. 3.0 ± 0.3 fold induction) (Fig. 2*C*). Therefore, when FcRγ was deleted, the presence of SAP did not reduce the appearance of monocyte-derived, spindle-shaped, fast proliferating fibroblasts found in association with I/RC.

Cardiac Function. As described previously, I/RC induced global ventricular dysfunction in wild-type mice that was inhibited by SAP treatment (6). We now found that treatment of FcRγ$^{-/-}$

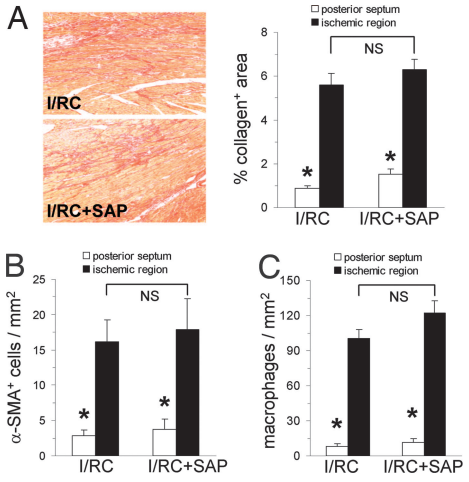

Fig. 1. FcRγ$^{-/-}$ mouse: histology. FcRγ$^{-/-}$ mice underwent 7 days of I/RC with or without SAP administration. (*A–C*) Tissue sections were stained for collagen (graph: $n = 5/6$ per group) (*A*), α-SMA ($n = 7$ per group) (*B*), and macrophages ($n = 8/9$ per group) (*C*). (Magnification: ×100.) Ischemic and nonischemic (posterior septum) regions were analyzed; the latter served as an interior control because this region should not be affected by I/RC. In contrast to wild-type mice (6), FcRγ$^{-/-}$ mice were not protected by SAP. SAP did not inhibit the interstitial deposition of collagen and did not diminish the amount of α-SMA$^+$ cells. However, consistent with our previous observation (6), SAP during I/RC given to either wild-type or FcRγ$^{-/-}$ mice did not reduce the number of macrophages. In sham-treated FcRγ$^{-/-}$ mice (with and without SAP treatment), no differences between ischemic and nonischemic regions were observed for collagen, α-SMA$^+$ cells, and macrophages (data not shown). *, $P < 0.05$ between ischemic and nonischemic groups; NS, not significant.

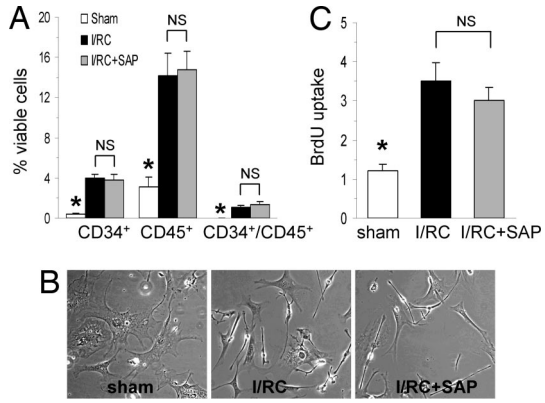

Fig. 2. FcRγ$^{-/-}$ mouse: isolated cell populations. FcRγ$^{-/-}$ mice underwent 5 days of I/RC with or without SAP administration. Hearts were removed, and cardiac fibroblasts were isolated. (*A*) Dispersed cells were analyzed for CD34 and CD45 expression on viable (calcein$^+$) cells by flow cytometry. Note that in FcRγ$^{-/-}$ mice undergoing I/RC, SAP did not reduce the number of CD34$^+$, CD45$^+$, and CD34$^+$/CD45$^+$ cells ($n = 7/8$ per group; *, $P < 0.05$ between sham and I/RC groups; NS, not significant), which was in contrast to our previous results using wild-type mice (6). (*B*) The same cell suspensions were cultured *in vitro*, and morphology was determined by phase contrast microscopy. (Magnification: ×100.) Cell cultures from SAP-treated and nontreated FcRγ$^{-/-}$ mice undergoing I/RC showed similar morphologic characteristics (small, spindle-shaped), which were in contrast to cells obtained from sham hearts (big, flat). (*C*) Cell isolations from SAP-treated and nontreated FcRγ$^{-/-}$ mice after I/RC proliferated at similar rates, and no differences were observed ($n = 5/6$ per group; *, $P < 0.05$ between sham and I/RC groups; NS, not significant).

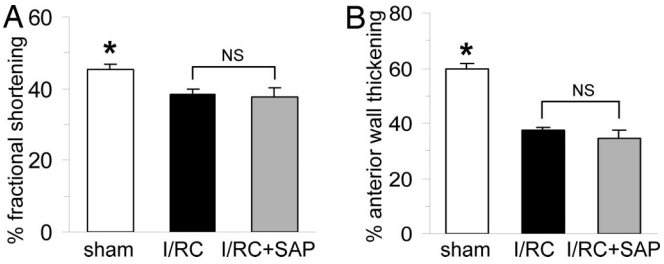

Fig. 3. FcR$\gamma^{-/-}$ mouse: cardiac function. FcR$\gamma^{-/-}$ mice underwent 7 days of I/RC with or without SAP administration. (*A* and *B*) SAP treatment of FcR$\gamma^{-/-}$ mice did not improve fractional shortening (*A*) and did not preserve anterior wall thickening (*B*) when compared with nontreated FcR$\gamma^{-/-}$ mice ($n = 8$ per group; *, $P < 0.05$ between sham and I/RC groups; NS, not significant). This finding was in contrast to our previous results in wild-type mice, in which SAP inhibited I/RC-mediated cardiac dysfunction (6).

mice with SAP did not prevent the development of I/RC-mediated myocardial dysfunction as manifested by reduced fractional shortening (38.5 ± 1.2 vs. 37.8 ± 2.4% FS) (Fig. 3*A*) and did not preserve cardiac structure as indicated by lesser anterior wall thickening (37.4 ± 1.3 vs. 34.6 ± 3.1% AWTh) (Fig. 3*B*). Therefore, FcR$\gamma^{-/-}$ mice were not protected by SAP from I/RC-induced cardiac dysfunction.

In Vitro* Model of Monocyte-to-Fibroblast Transition: Role of TEM.** ***Fibroblast formation. We found that a subpopulation of 10.0 ± 0.4% (Fig. 4*A*) of human adherent PBMCs matured into fibroblasts in the presence of 10% serum within 3 to 4 days after they were allowed to migrate through human umbilical vein endothelial cells (HUVECs) in response to MCP-1. Indeed, serum was necessary for this maturation; in the absence of serum, only 1.3 ± 0.1% of adherent cells became fibroblasts ($P < 0.01$, $n = 4$). We also found that no fibroblast formation occurred within 4 days in the presence of serum without TEM, which was consistent with previous reports (10). To further characterize the PBMC subpopulation that matured into fibroblasts, we isolated CD45$^+$/CD14$^+$ monocytes by magnetic bead separation and performed TEM. Our data show that an ≈95% pure CD45$^+$/CD14$^+$ mononuclear cell population (see Fig. 4*B*) resulted in a similar proportion of fibroblasts to macrophages (12.1 ± 1.1%) (Fig. 4*A*) as seen with the unseparated PBMC preparation, indicating that the cell population of interest was of CD45$^+$/CD14$^+$ monocytic origin. Monocyte-derived fibroblasts were characterized by their elongated morphology and contained cytoplasmic type I collagen. This phenotype contrasted with macrophages, which were round cells with central nuclei that lacked type I collagen (Fig. 4 *C* and *D*). After migration, cells expressing type I collagen had various morphologies ranging from oval cells with eccentric nuclei to fully fibroblastoid elongated cells with oval nuclei (Fig. 4 *E–G*). In the oval cells, collagen was confined to a perinuclear location typical of the Golgi apparatus, whereas in the fibroblastoid cells, collagen was detected throughout the cytoplasm. The cell in Fig. 4*H* with two nuclei may be dividing or may be binucleate as are many fibroblasts in culture.

MCP-1 promotes migration. Previously, we showed that MCP-1 represented an obligate pathophysiological factor in the development of I/RC-induced fibrosis (5, 6). Therefore, and because the role of MCP-1 in mononuclear chemotaxis is extensively documented in the literature (see review in ref. 11), we postulated that MCP-1 would augment the presence of monocyte-derived fibroblasts in the subendothelial chamber. Our results show that, although some basal TEM and fibroblast formation did occur, the presence of MCP-1 at optimal concentrations (650 ng/ml) augmented the appearance of fibroblasts by 5.3 ± 0.5 fold ($P < 0.01$, $n = 3$). The optimal concentration of MCP-1 in this system was the same for monocyte migration and fibroblast appearance. Thus, it was possible that MCP-1-driven chemotaxis was sufficient to induce the genesis of fibroblasts from monocytes. To address this issue, we examined the migration of monocytes through an agarose gel in response to a similarly optimized gradient of MCP-1, but no endothelial barrier. We found that, in the absence of TEM, MCP-1 induced migration of PBMCs through agarose did not result in type I collagen expressing cells (data not shown).

Effect of SAP. To examine the effect of SAP on fibroblast differentiation in our TEM assay, we added SAP to the PBMC suspension before TEM. We found that the presence of SAP significantly diminished the amount of fibroblasts found after TEM to 8 ± 3% of that seen in the absence of SAP (Fig. 5*A*),

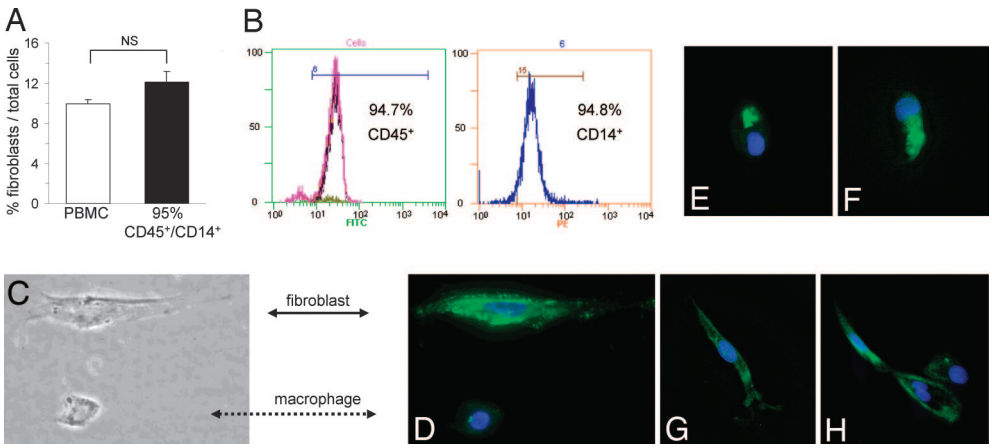

Fig. 4. *In vitro* cell identification. (*A*) Unseparated human PBMCs and ≈95% pure CD45$^+$/CD14$^+$ cell suspensions were allowed to migrate through HUVECs in response to MCP-1, and the number of cells in the bottom well were counted. Compared with the unseparated PBMC suspension, fibroblast formation did not diminish after removal of CD14$^-$ cells, indicating that monocytic CD45$^+$/CD14$^+$ cells held the subpopulation that developed into fibroblasts ($n = 4$; NS, not significant). (*B*) Representative cytometric diagrams showing that the CD45$^+$ mononuclear cell subpopulation (FITC-labeled) contained ≈95% CD14$^+$ (PE-labeled) cells. (*C*) Adherent cells in the bottom well were identified by morphology using phase contrast microscopy and (*D–H*) by type I collagen immunocytochemistry using fluorescence microscopy. (Magnification: ×200.) Macrophages were identified by their round shape, central nucleus, and lack of type I collagen (*C* and *D*, dotted arrow). Fibroblasts were identified by their elongated form and positive type I collagen expression (*C* and *D*, straight arrow, green). (*E–H*) Cells positive for type I collagen showing various stages of collagen expression were present by 4 days. Blue represents DAPI stain for nucleus identification.

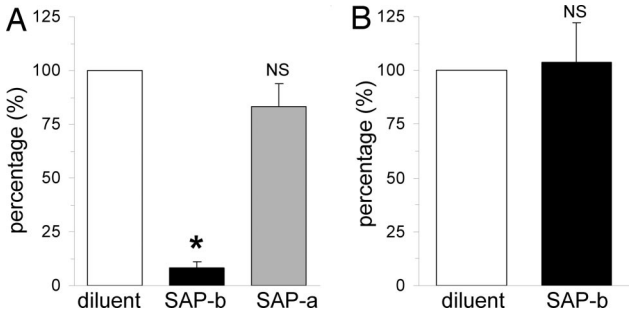

Fig. 5. *In vitro* effect of SAP on fibroblast formation. (*A*) Human PBMC migration through HUVECs was performed in response to MCP-1. Migration was performed in the absence of SAP (diluent) or in the presence of SAP in the top well before migration (SAP-b) or in the presence of SAP in the bottom well after migration (SAP-a). The formation of fibroblasts was inhibited only when SAP was present before TEM (SAP-b). Adding SAP after successful TEM did not inhibit maturation of fibroblasts ($n = 5$ per group; *, $P < 0.05$, compared with diluent and SAP-a groups; NS, not significant compared to diluent group). (*B*) PBMCs were allowed to migrate through HUVECs in response to MCP-1 in the absence or presence of SAP before TEM, but were collected in a collagen pad between the endothelial cell layer and the filter (pore size: 0.4 μm). The collagen pad was digested, and the total number of $CD45^+/CD14^+$ monocytes was counted by flow cytometry. The total amount of cells did not differ between diluent- and SAP-treated experiments ($n = 3$; NS, not significant).

indicating that SAP interfered with the assumption of the fibroblast phenotype from blood-borne precursor cells. However, when SAP was present only in the bottom well, formation of fibroblasts was not inhibited (83 ± 10% of that seen in the absence of SAP) (Fig. 5*A*). These data indicate that the critical point at which SAP exerted its effect on mononuclear cells was before or during endothelial transmigration. To determine whether the effect of SAP was exerted on the migration rather than subsequent maturation of fibroblast precursors, we counted the number of $CD45^+/CD14^+$ cells that transmigrated through HUVECs in the presence and absence of SAP in the top well. We found that the total number of monocytes in the bottom well did not differ between SAP- and diluent-treated conditions (100 vs. 104 ± 18%) (Fig. 5*B*), indicating that SAP inhibited the formation of fibroblasts from monocytes, rather than inhibiting their migration through the endothelial barrier.

Discussion

Nonadaptive Fibrosis and Inflammation. Augmented interstitial fibrosis of the heart almost invariably accompanies ventricular hypertrophy and failure and is considered an important pathophysiological factor in progressive cardiac dysfunction (12). Thus, "adverse remodeling" is generally considered to be one of the most important factors in the chronic and inexorable course of ventricular failure. The association of fibrotic ischemic cardiomyopathy with inflammation also has been widely studied and is considered to be multifactorial (13). However, although a variety of inflammatory cytokines and chemokines are implicated in this pathophysiological course, the cellular mechanism(s) by which inflammation contributes to fibrosis are not well understood.

In our previous work, we developed a model of fibrotic ischemic cardiomyopathy in the absence of cardiomyocyte death (I/RC) that resulted from daily ischemic episodes of 15 min duration (4). We suggested an important role for blood-borne, marrow-derived fibroblast precursors residing within the monocyte population that, when taken up into the heart by MCP-1-driven chemotaxis, underwent a transition into a small spindle-shaped population of myofibroblasts that expressed CD45 (hematopoietic marker) and CD34 (marker of primitive cells) (6). This I/RC-mediated injury could be prevented, both functionally and pathophysiologically, by overexpression of extracellular superoxide dismutase (4), genetic deletion of MCP-1 (5), and daily administration of SAP (6). In the current article, we wish to extend our observations to offer further insights into potential mechanisms of adverse remodeling associated with I/RC.

Monocyte-to-Fibroblast Transition. *In vitro* transition of cells within the monocyte population to a fibroblast-like cell ("fibrocytes") is well described in the literature (14). In general, incubation of the mononuclear cell population in the absence of serum results in the appearance of spindle-shaped cells expressing many fibroblast and myeloid markers within the first week; however, the presence of serum markedly retards this reaction (10, 15). When cells are incubated with serum, a similar transition has been reported to occur, but over a much longer incubation time (2–4 weeks) (10, 15). The work of Pilling *et al.* demonstrated that one factor in serum that retarded the development of fibrocytes was SAP (10). This observation led us to administer SAP to animals with I/RC (6). We observed that SAP administered *in vivo*, in doses compatible with those used *in vitro*, eliminated the appearance of marrow-derived, blood-borne fibroblast precursors.

Immune Modulation of the Cellular Mechanism of I/RC. The evidence for a relationship between the role of SAP on fibrocytes and on the development of I/RC was, although correlative, quite indirect. One problem was, for the monocyte to be the source of fibroblasts, they would have to rapidly undergo the transition in the presence of serum peaking within 5 days of the initiation of the I/RC protocol. In fact, peak MCP-1 levels in the myocardium were not reached until the third day, which would constrain the transition kinetics even further (4). In addition, the cellular mechanisms modulating the monocyte-to-fibroblast transition were not investigated. Therefore, we wished to examine further the regulatory functions of MCP-1 chemoattraction, cardiac uptake of fibroblast precursors, and SAP (which is known to bind to and activate FcRs) (9). Our observation that genetic deletion of FcRγ prevented the protective action of SAP in I/RC is strong evidence that SAP exerts its modulation of this process through its interaction with activating FcRs. Therefore, the current study provides strong evidence for a regulatory role of ligands that mediate monocyte-to-fibroblast transition through activating FcRs. Activation of FcRs is already a well known mechanism of modulating monocyte/macrophage phenotype, so there is a precedent that such a mechanism also might mediate monocyte-to-fibroblast transition (7, 8).

MCP-1. The CC chemokine MCP-1 is a well characterized chemoattractant for mononuclear cells that is elevated in chronic inflammatory diseases, in which the presence of those cells predominates (16). MCP-1 and its cognate receptor, CCR2, have been shown to play an important role in models of pulmonary, renal, and skin fibrosis (17–19). Overexpression of MCP-1 in murine hearts results in a dilated cardiomyopathy that is associated with intracellular fibrosis and monocyte infiltration (20). We have previously demonstrated that MCP-1 expression is elevated in human heart biopsies of ischemic cardiomyopathies in areas remote from the scar (21). The elevation of MCP-1 in the I/RC model precedes fibrosis and is prolonged for greater than 1 week, at which time fibrosis has peaked (4). When MCP-1 was genetically deleted, the monocytic and fibrotic reactions to I/RC were completely eliminated; there was no evidence of any compensatory elevation of other chemokines (5). Although MCP-1 is generally recognized only for its chemoattractant role, there have been reports and suggestions that it may directly influence fibroblast proliferation and differentiation, up-regulate collagen and TGFβ1 induction, and stimulate the

production of MMP-1 and TIMP-1 (22–24). To further pursue this notion, we examined the effect of MCP-1 stimulation on isolated cardiac fibroblasts from wild-type mice. Incubation of up to 16 h with a high concentration (100 ng/ml) resulted in no significant stimulation of fibrosis-associated genes (5). This finding leads us to suggest that the role of MCP-1 in I/RC resides in its chemoattractant action. Thus, to further understand the interaction among chemoattraction, FcR modulation, and transendothelial migration in the pathophysiology of I/RC, we developed an *in vitro* model in which we could incorporate and examine these factors individually.

TEM. Our *in vivo* data suggested that, at least in I/RC, MCP-1 is the pertinent chemoattractant (4, 5). They also suggested that a fibroblast precursor population of blood-borne origin appears in the heart (6). We therefore hypothesized that a subset of monocytic cells must differentiate into fibroblasts and must transmigrate across an endothelial barrier in response to MCP-1. To test this hypothesis *in vitro*, we used human PBMCs and HUVECs and demonstrated a rapid transition of monocytes to fibroblasts in 10% serum after TEM of the monocytes. Upon further characterization, we found that a $CD45^+/CD14^+$ cell subset of the PBMC preparation held the subpopulation that developed into fibroblasts, confirming previous studies suggesting that fibroblast precursors reside within the $CD14^+$ monocyte population (10). The transition was inhibited by exposure of monocytes to SAP during TEM, but not after successful TEM. Although TEM was largely MCP-1 dependent, MCP-1-induced migration through agarose (absence of endothelium) did not result in monocyte-to-fibroblast transition. Thus, accelerated monocyte-to-fibroblast transition in the presence of serum appears to follow TEM and occurs within the timeframe of fibroblast accumulation found in I/RC (6). The mechanism by which TEM exerts its cellular effect was not treated by these studies. However, the role of TEM in alteration of leukocyte phenotype is not unique. There is significant evidence in the literature of a variety of changes induced by TEM in both mononuclear and neutrophil cell populations (25, 26). Similarly, although the role of FcR in modulating monocyte phenotypes has been described previously (7, 8), their role in monocyte-to-fibroblast transition is unique, as is the fact that the FcR modulation must occur before TEM. A recent study described endothelial cells as a source of cardiac fibroblast formation via endothelial-to-mesenchymal transition (27). However, in I/RC, the agents that abrogate I/RC specifically eliminate the appearance of $CD45^+$ fibroblasts (6). In addition, the critical role of MCP-1 further suggests that, in this model, monocyte-derived fibroblasts are the dominant cellular agent (4, 5).

Conclusion

The development of an MCP-1-mediated, fibrotic cardiomyopathy in a murine model (I/RC) was inhibited by circulating SAP that suppressed the transition of a monocytic subpopulation into fibroblasts through action on its FcRs. Further *in vitro* analysis demonstrated that monocytes were required to migrate through endothelial cells to mature within a relevant timeframe into fibroblasts, and that SAP had to be present before endothelial transmigration to inhibit this maturation. Although there is ample evidence in the literature linking nonadaptive fibrosis to inflammatory signals in the heart, our results demonstrate a possible mechanism for this connection. Because the most common autocoidal associations connecting these two pathologies are TNFα and angiotensin II, and each of these has been associated with elevations in MCP-1 (28), it is possible that similar mechanisms of monocyte-to-fibroblast transition are also important for adverse remodeling of different etiologies. Such a possibility suggests the potential role for FcR activation in treatment of adverse remodeling and cardiac fibrosis.

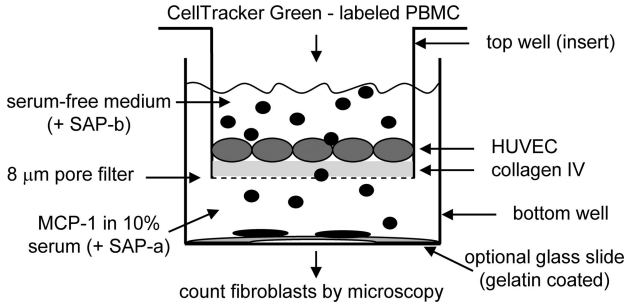

Fig. 6. Schematic outline of TEM. Top wells (inserts) with 8-μm pore filters were coated with human type IV collagen and seeded with HUVECs. Upon confluency, top wells were put into plastic bottom wells containing medium with 10% FBS and 650 ng/ml MCP-1. CellTracker Green-labeled human PBMCs in serum-free medium were placed into the top well. Some setups also received 10 μg of human SAP in either the top or bottom well. After 48 h, the inserts and nonadherent cells were removed, and new medium containing 10% serum was added to the bottom well. After 4 and 11 days of incubation, the number of adherent, fibroblast-shaped cells positive for CellTracker Green was determined under the microscope (and/or the total amount of all CellTracker Green positive cells). In some setups, gelatin-coated glass cover slips were placed into the bottom well that were removed after migration/incubation, and adherent cells were stained for type I collagen for identification.

Materials and Methods

I/RC. The 10- to 12-week-old FcRγ chain KO mice [FcR$\gamma^{-/-}$; Fcer1g (C57BL/6) mice; Taconic] were subjected to closed-chest surgery as previously described (4). One week after suture implantation, 15-min occlusions of the LAD were performed for 5 or 7 consecutive days, allowing a 24-h reperfusion period in between. Mice were euthanized 5 h after the last ischemic episode. All animals were treated in accordance with the guidelines of the Baylor College of Medicine Animal Care and Research Advisory Committee and with the rules governing animal use, as published by the National Institutes of Health.

SAP for *in Vivo* Administration. SAP was purified from mouse serum (Sigma–Aldrich) as described previously (6). Mice received a daily dose of 50 μg of murine SAP i.p. (I/RC + SAP group) or the equivalent molar dose (25 μg) of mouse albumin (Sigma–Aldrich) (I/RC group) 30 min before LAD occlusion.

Histology. To measure collagen deposition, paraffin-embedded tissue sections were stained with picrosirius red (Poly Scientific) and the images scanned (AxioCam HRc; Carl Zeiss). Collagen-stained areas were calculated as percentages of the total myocardial area by using Carl Zeiss IMAGE analysis software. Myofibroblast density (α-SMA^+ cells; antibody from Sigma–Aldrich) was determined as described previously, as was macrophage density (Mac-2^+ cells; antibody from Cedarlane) (21).

Cell Isolation. Cardiac fibroblasts were isolated by enzymatic digestion and cultured as described previously (6). For flow-cytometric analysis, 1×10^5 freshly isolated cells were incubated with 50 nM calcein (Invitrogen/Molecular Probes) and 0.5 μg of PE-conjugated CD34 or biotin-conjugated CD45 antibodies, followed by PE/Cy-5-conjugated streptavidin (BD Biosciences). Fluorescence intensities were measured on a Beckman Coulter Epics XL.MCL.

Proliferation. Proliferation of cultured cells was determined by BrdU incorporation as described previously (6). To normalize data from different experiments, enhanced proliferation in response to serum was expressed as the fold increase compared with cells maintained in serum-free medium.

Echocardiography. Echocardiography was performed before the first ischemic episode and after 7 days of I/RC. Data were obtained by 2D directed M-mode echocardiography as described previously (4) by using an Acuson Sequoia Cardiac System (C256). All images were digitally acquired and stored for off-line analysis. Fractional shortening and anterior wall thickening were calculated as previously described (4).

Normal Donor Blood. Blood was obtained from volunteers under a protocol approved by the Institutional Review Board of Baylor College of Medicine. Blood anticoagulated with citrate-phosphate-dextrose solution (Sigma–Aldrich) was fractionated by Ficol-Hypaque gradient centrifugation

(Histopaque-1077; Sigma–Aldrich) to collect mononuclear cells. To enrich $CD45^+/CD14^+$ cells, PBMCs (3×10^6 cells) were incubated with 40 μg of human IgG (Sigma–Aldrich) to block nonspecific binding before the addition of anti-CD14 magnetic beads (Miltenyi Biotec). Separation was performed by using an AutoMACS magnetic cell sorter (Miltenyi Biotec). After separation, cells were stained with PE-conjugated anti-CD14 and FITC-conjugated anti-CD45 antibodies (Beckman Coulter), and fluorescence intensities were measured on a Beckman Coulter Quanta SC MPL cytometer.

TEM. HUVECs were obtained from Dr. C. W. Smith (Baylor College of Medicine) and used at passages 1–6. They were grown in M199 (Invitrogen) with 10% fetal and 10% adult bovine serum (HyClone), 50 μg/ml heparin (Sigma–Aldrich), and 50 μg/ml endothelial cell growth supplement (BD Biosciences). For a TEM assay, inserts (membrane pore size: 8 μm; Corning) were coated overnight with 1 μg of human type IV collagen (Chemicon), and HUVECs were seeded at ≈40,000 cells per insert. HUVECs were grown to postconfluency (4–7 days). Human PBMCs ($5–25 \times 10^4$) or its $CD45^+/CD14^+$ subpopulation (12×10^4) labeled with CellTracker Green (Invitrogen/Molecular Probes) were added to the top (insert) well in RPMI 1640 (Invitrogen) with 1% ITS-3 (Sigma–Aldrich). RPMI 1640 with 10% FBS was added to the well below. MCP-1 (650 ng/ml; R&D Systems) or diluent (0.1% HSA in PBS; Mediatech) was added to the bottom well for chemoattraction (see Fig. 6). Some setups received human SAP (10 μg rhPTX2; R&D Systems) in either the top or bottom well. PBMCs were allowed to migrate for 48 h and then the inserts and nonadherent cells in the bottom wells were removed. At day 4, the number of CellTracker $Green^+$, fibroblast-shaped cells and total cells were counted. Each donor's cells were measured in triplicate. Due to differences in absolute numbers between PBMC donors, the number of cells in the experimental well (SAP, MCP-1, or serum) was divided by the number in the corresponding control well (diluent) to normalize the data.

Immunofluorescence. After TEM, cells were cultured on 2% gelatin (Sigma–Aldrich) coated glass cover slips for 3–11 days. The cells were fixed and permeabilized, and unspecific binding was blocked by 10 mg/ml human IgG (Sigma–Aldrich). Cells were stained with anti-type I collagen (Rockland), followed by FITC-conjugated anti-rabbit antibody (BD Biosciences). Microscopy was performed on an Olympus CKX41 (phase contrast), an Olympus AX-70 (fluorescence), or on a Delta Vision Spectris (fluorescence; Applied Precision), from which z-stack images were deconvolved by using soft-WoRx.

TEM into Collagen Pads. Inserts (membrane pore size: 0.4 μm) were layered with 50% hydrated collagen pads (Vitrogen 100; Cohesion) coated with type IV collagen and HUVECs were seeded. PBMCs were added to the top well and 650 ng/ml MCP-1 to the bottom. After 48 h, nonadherent PBMCs and HUVECs were removed by brief trypsin treatment. The collagen pads were digested by Liberase 2 (Roche Applied Science). The released cells were stained with fluorochrome-labeled antibodies against CD45 and CD14 (Beckman Coulter), and the number of $CD45^+$, $CD14^+$ cells was counted on a Beckman Coulter Quanta by using Cell Lab Quanta SC MPL software.

Migration Through Agarose. The under agarose chemotaxis assay protocol was modified from a report by Heit (29). Briefly, a single-chambered glass slide/vessel (BD Biosciences) was coated with 2% gelatin. Then 1% agarose (type VII; Sigma–Aldrich) in RPMI 1640/10% FBS was poured onto the slide to form a pad. Two wells were cut into the pad. PBMCs (2×10^5in 10 μl) were loaded into one well and 75 nM MCP-1 (in 10 μl) into the other well. Twelve hours later, the entire slide was flooded with warm medium to dilute the chemotactic agent and feed the cells. After 3 further days of incubation, the slide was fixed with methanol, the agarose pad was peeled off, and the attached cells were stained for type I collagen.

Statistical Analysis. All data are expressed as mean ± SEM. A two-tailed, unpaired Student's *t* test was used to determine a significant difference between two groups. One-way ANOVA was used to evaluate differences between three or more groups. Post hoc testing (Tukey–Kramer method) was performed when appropriate. A P value <0.05 was considered statistically significant.

ACKNOWLEDGMENTS. We thank Thuy Pham, Stephanie Butcher, and Geoffrey Bender for expert technical assistance; Dr. Richard Gomer (Rice University) for his insights and contribution of purified mouse SAP; and Varsha Vahil for its preparation. This work was supported by National Heart, Lung, and Blood Institute Grants HL42550, R01 HL076661, HL089792, T32HL107816, and R01 HL083029; the Medallion Foundation; and The Methodist Hospital Foundation.

1. Sun Y, Weber KT (2005) Animal models of cardiac fibrosis. *Methods Mol Med* 117:273–290.
2. Frangogiannis NG, *et al*. (2002) Active interstitial remodeling: An important process in the hibernating human myocardium. *J Amer College Cardiol* 39:1468–1474.
3. Sun Y, Weber KT (1998) Cardiac remodelling by fibrous tissue: Role of local factors and circulating hormones. *Ann Med 30 Suppl* 1:3–8.
4. Dewald O, *et al*. (2003) Development of murine ischemic cardiomyopathy is associated with a transient inflammatory reaction and depends on reactive oxygen species. *Proc Natl Acad Sci USA* 100:2700–2705.
5. Frangogiannis NG, *et al*. (2007) Critical role of monocyte chemoattractant protein-1/CC chemokine ligand 2 in the pathogenesis of ischemic cardiomyopathy. *Circulation* 115:584–592.
6. Haudek SB, *et al*. (2006) Bone marrow-derived fibroblast precursors mediate ischemic cardiomyopathy in mice. *Proc Natl Acad Sci USA* 103:18284–18289.
7. Nimmerjahn F, Ravetch JV (2008) Fcgamma receptors as regulators of immune responses. *Nat Rev Immunol* 8:34–47.
8. Ivan E, Colovai AI (2006) Human Fc receptors: Critical targets in the treatment of autoimmune diseases and transplant rejections. *Hum Immunol* 67:479–491.
9. Bharadwaj D, Mold C, Markham E, Du Clos TW (2001) Serum amyloid P component binds to Fc gamma receptors and opsonizes particles for phagocytosis. *J Immunol* 166:6735–6741.
10. Pilling D, Buckley CD, Salmon M, Gomer RH (2003) Inhibition of fibrocyte differentiation by serum amyloid P. *J Immunol* 171:5537–5546.
11. Xia Y, Frangogiannis NG (2007) MCP-1/CCL2 as a therapeutic target in myocardial infarction and ischemic cardiomyopathy. *Inflamm Allergy Drug Targets* 6:101–107.
12. Weber KT, Brilla CG, Janicki JS (1993) Myocardial fibrosis: Functional significance and regulatory factors. *Cardiovasc Res* 27:341–348.
13. Frangogiannis NG (2004) Chemokines in the ischemic myocardium: From inflammation to fibrosis. *Inflamm Res* 53:585–595.
14. Quan TE, Cowper S, Wu SP, Bockenstedt LK, Bucala R (2004) Circulating fibrocytes: Collagen-secreting cells of the peripheral blood. *Int J Biochem Cell Biol* 36:598–606.
15. Abe R, Donnelly SC, Peng T, Bucala R, Metz CN (2001) Peripheral blood fibrocytes: Differentiation pathway and migration to wound sites. *J Immunol* 166:7556–7562.
16. Charo IF, Taubman MB (2004) Chemokines in the pathogenesis of vascular disease. *Circ Res* 95:858–866.
17. Smith RE, *et al*. (1995) A role for C-C chemokines in fibrotic lung disease. *J Leukoc Biol* 57:782–787.
18. Inoshima I, *et al*. (2004) Anti-monocyte chemoattractant protein-1 gene therapy attenuates pulmonary fibrosis in mice. *Am J Physiol Lung Cell Mol Physiol* 286:L1038–L1044.
19. Ferreira AM, *et al*. (2006) Diminished induction of skin fibrosis in mice with MCP-1 deficiency. *J Invest Dermatol* 126:1900–1908.
20. Kolattukudy PE, *et al*. (1998) Myocarditis induced by targeted expression of the MCP-1 gene in murine cardiac muscle. *Am J Pathol* 152:101–111.
21. Frangogiannis NG, *et al*. (2002) Evidence for an active inflammatory process in the hibernating human myocardium. *Amer J Pathol* 160:1425–1433.
22. Kruglov EA, Nathanson RA, Nguyen T, Dranoff JA (2006) Secretion of MCP-1/CCL2 by bile duct epithelia induces myofibroblastic transdifferentiation of portal fibroblasts. *Am J Physiol Gastrointest Liver Physiol* 290:G765–G771.
23. Yamamoto T, Eckes B, Mauch C, Hartmann K, Krieg T (2000) Monocyte chemoattractant protein-1 enhances gene expression and synthesis of matrix metalloproteinase-1 in human fibroblasts by an autocrine IL-1 alpha loop. *J Immunol* 164:6174–6179.
24. Gharaee-Kermani M, Denholm EM, Phan SH (1996) Costimulation of fibroblast collagen and transforming growth factor beta1 gene expression by monocyte chemoattractant protein-1 via specific receptors. *J Biol Chem* 271:17779–17784.
25. McGettrick HM, *et al*. (2006) Chemokine- and adhesion-dependent survival of neutrophils after transmigration through cytokine-stimulated endothelium. *J Leukoc Biol* 79:779–788.
26. Borregaard N, Sorensen OE, Theilgaard-Monch K (2007) Neutrophil granules: A library of innate immunity proteins. *Trends Immunol* 28:340–345.
27. Zeisberg EM, *et al*. (2007) Endothelial-to-mesenchymal transition contributes to cardiac fibrosis. *Nat Med* 13:952–961.
28. Mann DL (2003) Stress-activated cytokines and the heart: From adaptation to maladaptation. *Annu Rev Physiol* 65:81–101.
29. Heit B, Kubes P (2003) Measuring chemotaxis and chemokinesis: The under-agarose cell migration assay. *Sci STKE* 2003:L5.